Published in final edited form as:
Exp Gerontol. 2008 April ; 43(4): 275–285. doi:10.1016/j.exger.2007.12.004.

A model on the influence of age on immunity to infection with *Mycobacterium tuberculosis*

Avner Friedman[1,2], **Joanne Turner**[3], and **Barbara Szomolay**[1]

1 *Mathematical Biosciences Institute, The Ohio State University*

2 *Department of Mathematics, The Ohio State University*

3 *Center for Microbial Interface Biology, Department of Internal Medicine, The Ohio State University*

Abstract

Increasing susceptibility of the elderly to many infectious diseases is highly associated with the loss or delay in the generation of antigen specific $CD4^+$ T cells. For *Mycobacterium tuberculosis*, where antigen-specific $CD4^+$ T cell derived IFN-γ is essential, such a loss can lead to a significant failure to control infection. The present paper develops a mathematical model of infection with *M. tuberculosis* in old mice. The model includes an early resistance to infection which is mediated by $CD8^+$ T cells. A subsequent reversal of this phenotype results from the slow generation of $CD4^+$ T cell mediated immunity in old age. The model simulations corroborate experimental data and hence, the model was used to test whether immunity to infection could be improved in old mice, if $CD4^+$ T cell responses were enhanced. Our simulations indicate that boosting antigen presentation and T cell proliferation can decrease the *M. tuberculosis* burden in the lung.

1 Introduction

Nearly every component of the immune system undergoes age-associated changes. The most significant are thymic atrophy and an increase in the proportions of antigen experienced (memory) cells in the periphery [7]. The accumulation of antigen experienced cells in the periphery can lead to aberrations in cell function that likely have significant biological consequences. Most significant are the changes that occur within the $CD4^+$ T cell compartment. $CD4^+$ T cell function is markedly impaired with a reported decrease in the amount of IL-2 produced in response to antigen [8], [11]. Poor generation of antigen specific $CD4^+$ T cell responses is thought to contribute to increased susceptibility to *Mycobacterium tuberculosis* infection in mice [13], [14]. Despite such susceptibility, in the mouse model it has also been shown that old mice possess a population of highly activated $CD8^+$ T cells that can secrete IFN-γ in an antigen independent manner [23], [26]. These $CD8^+$ T cells contribute to an early control of *M. tuberculosis* infection within the lung. This early control is transient, and old mice eventually succumb to infection [13].

Control of an infection with *M. tuberculosis* requires the generation of IFN-γ secreting antigen specific $CD4^+$ T cells, and activation of infected macrophages that can subsequently limit bacterial growth [5]. In old age, the generation of antigen specific $CD4^+$ T cell mediated immunity is delayed or impaired [14] and it is thought that poor $CD4^+$ T cell mediated immunity

contributes to the increased susceptibility of the elderly to develop tuberculosis [2]. Indeed, the elderly make up approximately one fifth of all tuberculosis cases in the US [17]. Tuberculosis in the elderly can occur through reactivation of a previously latent infection or from primary infection [18], [21]. Primary infection occurs when elderly individuals encounter *M. tuberculosis* for the first time, an event that often occurs in the nursing home environment. Under these circumstances, with waning immunity, the elderly are highly susceptible to developing tuberculosis [18], [21]. This study will model primary tuberculosis in young and old mice, as a model of primary infection in human. The aged murine model has been used extensively and is an accepted model to study the influence of increasing age on immunity. Furthermore, like human, old mice are more susceptible to primary infection with *M. tuberculosis* [13].

In this paper we develop a mathematical model for control of *M. tuberculosis* infection in the lungs of young (3 month) and aged (18 month) animals. The model includes the early participation of $CD8^+$ T cells which have been shown to secrete IFN-γ in an antigen independent manner and are associated with an early resistance to infection, leading to an initial reduction in the bacterial load within the lung [26]. IFN-γ is essential for control of *M. tuberculosis* infection, which has been explicitly demonstrated in mouse models and in human [6], [10]. In old mice however, IFN-γ can be detected within the lung much earlier and in greater amounts than in young mice; is secreted by $CD8^+$ T cells, and is thought to provide an innate function to stimulate macrophage activation, leading to better early control of infection [23]. The model we propose also accounts for the delayed or slower generation of antigen specific $CD4^+$ T cells that has been reported in old mice in response to infection with *M. tuberculosis* [23], [14]. This delay contributes to the subsequent increased bacterial load seen within the lungs of old mice and is considered to be the primary defect for increased susceptibility to infection with this pathogen.

Mathematical models of *M. tuberculosis* infection in humans and mice were developed by Wigginton et al. [29] and Sud et al. [19]. Although these models are quite comprehensive, they do not address the effect of increasing age on the development of tuberculosis disease. To focus on the effects of aging, our model includes only the cell populations and cytokines which play the most significant role in the control of an infection with *M. tuberculosis* [3], [6], [22], [16], [20], and those that significantly change with increasing age [8]. Using these variables, we compared the progression of *M. tuberculosis* infection in old versus young mice. We demonstrate that our simulations corroborate experimental data and provide a model that can be used as a computational tool to test hypotheses on how the immune system can be manipulated in the elderly to improve the prognosis of infectious diseases.

2 The Mathematical Model

All variables used in the mathematical model are listed in Table 1. In what follows, we give a brief description of the bacterial, macrophage and T cell populations presented in the model.

Macrophages are defined in one of three states: infected, activated or resting. Activated macrophages are capable of controlling mycobacterial growth and presenting antigen to T cells via MHCI and MHCII [5]. A resting macrophage becomes activated by a small number n_2 (taken to be 5) of bacteria in the presence of IFN-γ. IFN-γ stimulates the activated macrophage to limit *M. tuberculosis* growth and the bacterial numbers remain low. For simplicity, our model indicates that T cell derived IFN-γ is sufficient for macrophage activation however we acknowledge that macrophages require additional signals, such as TNF or high bacillary burden, to become activated [5]. A resting macrophage becomes an infected macrophage when it is infected (by n_3 bacteria, taken to be 10) in the absence of IFN-γ. A failure to activate the macrophage with IFN-γ leads to increased intracellular growth of *M. tuberculosis*. An infected

macrophage fails to control mycobacterial growth and can burst when it exceeds its maximal carrying capacity of N (taken to be 25) mycobacteria; the average number of mycobacteria in an infected macrophage is denoted by n_1 (taken to be 20). We assume that infected macrophages can present antigen via MHCI, but MHCII presentation is inefficient. The number of resting macrophages remains unchanged during the progression of the disease, i.e., when some resting macrophages become activated or infected, new ones come to replace them. We assume that infected macrophages can become activated by IFN-γ.

The bacterial population is divided according to whether they reside within infected or activated macrophages (intracellular), or whether they are located outside the macrophage (extracellular). The number of extracellular bacteria is relatively small for both young and old mice, since extracellular growth of mycobacteria is considered to be negligible. The bacterial growth of bacteria residing within activated macrophages is assumed to be nearly negligible.

Our model includes $CD4^+$ and $CD8^+$ T cells. For simplicity, we do not include other cells, such as naive T cells as used in [19]. A brief schematic guide to our mathematical model is given in Figure 1. Activated and infected macrophages secrete interleukin 12 (IL-12) which, combined with antigen presentation via MHC, activates $CD4^+$ and $CD8^+$ T cells. In the presence of IL-12 and MHC both $CD4^+$ and $CD8^+$ T cells secrete antigen-specific IFN-γ which activates macrophages. For old mice, IL-12 can activate $CD8^+$ T cells directly. $CD4^+$ T cells secrete IL-2 which further enhances T cell responses. Activated macrophages can secrete interleukin 10 (IL-10) which can deactivate activated macrophages to become infected macrophages.

2.1 The model equations

Bacterial dynamics—The equations for bacterial dynamics are given by Eqs. (1)-(3).

$$\frac{dB_I}{dt} = \underbrace{\alpha_I B_I\left(1 - \frac{B_I^2}{B_I^2 + (NM_I)^2}\right)}_{\text{growth}} + \underbrace{k_1 n_3 M_R \frac{B_E}{B_E + c_1}}_{\text{gain of } B_I \text{ due to infection of } M_R \text{ at a threshold of } n_3 \text{ bacteria}} - \underbrace{k_2 N M_I \frac{B_I^2}{B_I^2 + (NM_I)^2}}_{\text{loss of } B_I \text{ due to burst}} - \underbrace{n_1 k_3 B_I \frac{I_\gamma}{I_\gamma + c_2}}_{\text{loss due to activation}} + \underbrace{n_2 k_4 B_A \frac{I_{10}}{I_{10} + c_3 I_\gamma + c_4}}_{\text{gain due to deactivation}} \tag{1}$$

$$\frac{dB_A}{dt} = \underbrace{\alpha_A B_A}_{\text{growth}} - n_2 k_4 B_A \frac{I_{10}}{I_{10} + c_3 I_\gamma + c_4} + n_1 k_3 B_I \frac{I_\gamma}{I_\gamma + c_2} - \underbrace{n_2 \mu_{MA} B_A}_{\text{loss due to death of } M_A} \tag{2}$$

$$\frac{dB_E}{dt} = \underbrace{\alpha_E B_E}_{\text{growth}} - k_1 n_3 M_R \frac{B_E}{B_E + c_1} + k_2 N M_I \frac{B_I^2}{B_I^2 + (NM_I)^2} - \underbrace{k_5 M_A B_E}_{\text{take up by } M_A} + n_2 \mu_{MA} B_A \tag{3}$$

Explanation: Bacteria inside the infected macrophages grow at a maximal rate of α_I, reduced by a logistic Hill kinetics with a parameter depending on the maximal carrying capacity of N bacteria in an infected macrophage. A resting macrophage becomes infected at an assumed threshold of n_3 bacteria, and hence, it represents a gain term for the intracellular bacteria. The

third term on the right-hand side of Eq. (1) accounts for the release of intracellular bacteria due to lysis (burst) of infected macrophages. The fourth and fifth terms represent the exchange between B_I and B_A due to activation of infected macrophages by IFN-γ and deactivation of activated macrophages by IL-10. In Eq. (2), bacteria inside the activated macrophages grow at a maximal rate of α_A and lose n_2 bacteria on average at a rate of μ_{MA} due to death of their host macrophage. In Eq. (3), extracellular bacteria grow at a rate of α_E and are taken up by activated macrophages at a rate of k_5. Following an experimental infection with *M. tuberculosis*, we have previously shown that uptake of bacteria is the same for old and young mice [26].

Macrophage dynamics—The equations describing the rates of changes for macrophage populations are given by Eqs. (4)-(5).

$$\frac{dM_I}{dt} = \underbrace{k_1 M_R \frac{B_E}{B_E + c_1}}_{\text{infection of } M_R} - \underbrace{k_2 M_I \frac{B_I^2}{B_I^2 + (NM_I)^2}}_{\text{burst}} \underbrace{- k_3 M_I \frac{I_\gamma}{I_\gamma + c_2}}_{\text{activation}} + \underbrace{k_4 M_A \frac{I_{10}}{I_{10} + c_3 I_\gamma + c_4}}_{\text{deactivation}} - \underbrace{\mu_{MI} M_I}_{\text{death}} \tag{4}$$

$$\frac{dM_A}{dt} = - k_4 M_A \frac{I_{10}}{I_{10} + c_3 I_\gamma + c_4} + k_3 M_I \frac{I_\gamma}{I_\gamma + c_2} - \underbrace{\mu_{MA} M_A}_{\text{death}} + \underbrace{k_6 M_R \frac{B_E}{B_E + c_5} \frac{I_\gamma}{I_\gamma + c_6}}_{\text{activation of } M_R} \tag{5}$$

Explanation: In Eq. (4) the first term accounts for infection of resting macrophages; the second term accounts for bursting of infected macrophages; the remaining three terms account for activation of infected macrophages by IFN-γ, deactivation of activated macrophages by IL-10, and the death of infected macrophages. The first two terms in Eq. (5) are exchanges with infected macrophages, and the last term accounts for activation of resting macrophages by extracellular bacteria in the presence of IFN-γ.

Cytokine dynamics—The equations of cytokine dynamics are given by Eqs. (6)-(9).

$$\frac{dI_{10}}{dt} = \underbrace{k_7 M_I \frac{c_7}{I_{10} + c_7}}_{\text{IL-10 production by } M_I} - \underbrace{\mu_{10} I_{10}}_{\text{decay}} \tag{6}$$

$$\frac{dI_{12}}{dt} = \underbrace{k_8 M_A \frac{c_8}{I_{10} + c_8}}_{\text{IL-12 production by } M_A} + \underbrace{k_9 M_R \frac{B_E}{B_E + c_9}}_{\text{IL-12 production by } M_R} - \underbrace{\mu_{12} I_{12}}_{\text{decay}} \tag{7}$$

$$\frac{dI_2}{dt} = \underbrace{k_{10} T_4}_{\text{IL-2 production}} - \underbrace{(k_{11} T_4 + k_{12} T_8) \frac{I_2}{I_2 + c_{10}}}_{\text{loss due to proliferation of T cells}} - \underbrace{\mu_2 I_2}_{\text{decay}} \tag{8}$$

$$\frac{dI_\gamma}{dt} = \underbrace{\left(\lambda_u(t)\,T_4 + \lambda_y(t)\,T_8\right)\frac{I_{12}}{I_{12}+c_{11}}}_{\text{IFN}-\gamma \text{ production by CD4}^+ \text{ and CD8}^+} - \underbrace{\mu_\gamma I_\gamma}_{\text{decay}} \tag{9}$$

Explanation: IL-10 and IL-12 are produced by infected and activated macrophages at rates of k_7 and k_8, respectively, but both processes are inhibited by IL-10. In addition, IL-12 is produced by resting macrophages in response to infection at a rate of k_9. In old mice, increased IL-12 is detected in the lung early after infection with *M. tuberculosis* [26]. IL-2 is secreted by $CD4^+$ T cells and is consumed by activated $CD4^+$ and $CD8^+$ T cells. IL-2 secretion by $CD4^+$ T cells is reportedly decreased in old age [8], [11]. IFN-γ is secreted by $CD4^+$ and $CD8^+$ T cells in the presence of IL-12; this production is time-dependent. In young mice, antigen specific IFN-γ production by $CD4^+$ and $CD8^+$ T cells is detectable 2 weeks after infection, and reaches a maximal level after 3 weeks.

In old mice, $CD8^+$. T cells can secrete IFN-γ in an antigen dependent manner which is dependent on IL-12 [26]. Furthermore, increased IFN-γ is detected within the lungs of old mice early after infection with *M. tuberculosis* [26]. Therefore, $CD8^+$ T cells derived IFN-γ is reported as early as 2 weeks post infection. Based upon experimental evidence [23], antigen dependent IFN-γ production by $CD8^+$ and $CD4^+$ T cells is not detected until the third week of infection in old mice and IFN-γ production in young mice is somewhat higher than that of old mice.

T cell dynamics—T cell densities evolve by Eqs. (10)-(11).

$$\frac{dT_4}{dt} = \underbrace{\lambda_z(t)\,M_A I_{12}}_{\text{MHCII activation}} + \underbrace{k_{13}T_4\frac{I_2}{I_2+c_{10}}}_{\text{proliferation by IL}-2} - \underbrace{\mu_{T4}T_4}_{\text{decay}} \tag{10}$$

$$\frac{dT_8}{dt} = \underbrace{\lambda_x(t)\,(M_A+M_I)\,I_{12}}_{\text{MHCI activation}} + \underbrace{k_{14}T_8\frac{I_2}{I_2+c_{10}}}_{\text{proliferation by IL}-2} - \underbrace{\mu_{T8}T_8}_{\text{decay}} \tag{11}$$

Explanation: We do not write explicitly the concentration of MHCI, MHCII in Eqs. (10)-(11), since we assume that they are uniformly distributed on the membrane of macrophages and thus depend only on t. Hence, we take the rate of MHCII activation to be a time dependent function $\lambda_z(t)$. Similarly, we take the rate of MHCI activation to be a time dependent function $\lambda_x(t)$. IL-12 combined with antigen presented in the context of MHCII stimulates $CD4^+$ T cells to proliferate, thereby expanding the $CD4^+$ T cell population. IL-12 combined with MHCI/antigen increases the number of $CD8^+$ T cells.

3 Parameter values

Table 2 lists the model parameters and their explanation. Table 3 gives the parameter values of the differential equations (1)-(11) for young and old mice. The last column gives the reference to experimental data. When no such data are available, we estimated the parameters and made adjustments to align with experimental results reported in [23], [26], [27], [28], [9]. Our numerical simulations start at day 7 of infection; they will be discussed in the next section.

The death rates of macrophages (μ_{MI}, μ_{MA}) are based on the assumption that the life span of infected macrophages is 7 days, and 90 days for activated macrophages. Bacteria inside infected macrophages are assumed to divide every 24 hours. The parameters in the last four

rows of Table 3 are labelled with a 'star' to indicate that these are the base values for the time-dependent coefficients $\lambda_u(t)$, $\lambda_y(t)$, $\lambda_z(t)$, $\lambda_x(t)$, namely, their values after 3 weeks of infection.

Some of the parameters listed in Table 3 differ for young and old mice. These differences are based on experimental evidence as cited, extrapolated from experimental evidence from non-infectious studies, or unpublished observations. The percentage difference between the parameters for old and young mice is based upon experimental data (when available) or extrapolated for the best fit (range 10%-130%).

Activation of resting macrophages by IFN-γ in response to infection is larger for old mice ($k_{3,o} > k_{3,y}$). This increase is based upon the early and increased production of IFN-γ and IL-12 and in the lungs of old mice in response to infection (ref. [26]), and unpublished observations demonstrating that macrophages from the lungs of old mice secrete more IL-12 upon infection with *M. tuberculosis in vitro* (data not shown).

The production rate of IL-10 by infected macrophages and the production rate of IL-12 by activated macrophages is larger for old mice ($k_{7,o} > k_{7,y}$ and $k_{8,o} > k_{8,y}$). The production rate of IL-12 by resting macrophages in response to infection is larger for old mice ($k_{9,o} > k_{9,y}$) ([26] and unpublished observations).

The production rate of IL-2 by $CD4^+$ T cells is larger for young mice ($k_{10,o} < k_{10,y}$)([4]). Deficiencies in IL-2 production in old age have been well documented in the literature [8], [11] and reduced IL-2 production has been observed in *M. tuberculosis* infected old mice (unpublished observations).

IL-2 is lost as it is consumed by activated $CD4^+$ and $CD8^+$ T cells and this loss is larger for young mice ($k_{11,o} < k_{11,y}$), due to the increased number of activated T cells present within the lung. In addition, CD^+ and $CD8^+$ T cell numbers are enhanced by IL-2, and this gain is larger for young mice ($k_{13,o} < k_{13,y}$ and $k_{14,o} < k_{14,y}$) ([8]).

The rate of IFN-γ production by $CD8^+$ T cells is $\lambda_y(t)$ and the rate of IFN-γ production by $CD4^+$ T cells is $\lambda_u(t)$. The profile of $\lambda_y(t)$ and $\lambda_u(t)$ for young and old mice is shown in Figure 2. $CD8^+$ T cell derived IFN-γ is initially greater in old mice, as demonstrated experimentally [26]. However, antigen independent secretion of IFN-γ is transient and subsequently dissipates. At this time, young mice have generated antigen specific $CD8^+$ T cells that can secrete IFN-γ. In contrast, the generation of antigen specific $CD8^+$ T cells is delayed in old age ([14] and unpublished observations). Therefore, at the end of week 2 of infection in old mice, the production of IFN-γ falls off significantly, with a slight overshoot.

The rate of IFN-γ production by $CD4^+$ T cells is $\lambda_u(t)$. For old mice, $CD4^+$ T cells start producing antigen specific IFN-γ at day 21 and, for young mice, at day 14, reflecting the delay in generation of antigen specific immunity in old mice [23]. The rate for IFN-γ production in young mice stabilizes after day 21, whereas for old mice, there is an additional one week delay. These data have been verified experimentally [23].

Macrophages within the lung can present antigen throughout infection, however the generation of IFN-γ, and expansion of T cells, is dependent on antigen specific T cells being present within the lung. Here we link the antigen specific response to MHC. Hence, we take the time-dependent MHC activation rates $\lambda_z(t)$ and $\lambda_x(t)$ to be zero before day 14 (or day 21 in case of $\lambda_z(t)$ for old mice) and constant otherwise; see Figure 2.

The bacterial load within the lungs of young and old mice is initially different. Early during infection old mice have more IFN-γ and IL-12 within the lung which leads to enhanced macrophage activation. Activation of macrophages for old mice is greater during the first 10-14

days. Hence, initially the number of activated macrophages is larger and the number of infected macrophages is lower for old mice. As described above, cytokine production (IL-12 and IFN-γ) in aged mice is elevated, with the exception of IL-2. This early activation results in an early reduction of the bacteria load in the lung compared to young mice. Hence, we take the total number of bacteria at day 7 to be lower for old mice.

4 Simulation Results

In this section we describe simulation results based on our model and compare these results with experimental measurements. The simulation results did not change qualitatively if the average numbers of bacteria (n_1, n_2 and n_3) inside the macrophages were either increased by up to 100% or decreased by 50%.

Figure 3 simulates the bacterial load for both young and old mice. Because old mice have an early burst of IFN-γ /IL-12 in response to infection, leading to macrophage activation, the bacterial load is initially smaller for old mice. After 21 days, however, this reverses and the bacterial load for old mice becomes larger. This cross-over is accounted for by the delayed generation of antigen specific $CD4^+$ and $CD8^+$ T cell responses in old mice and continued growth of *M. tuberculosis* in the lung. Both loads stabilize after 45 days and, due to the delayed antigen specific responses, the bacterial load for old mice remains twice as high as for young mice. The extracellular bacteria are approximately 5% of the total load (not shown here). The simulation results agree with experimental measurements in [23], [26], [4].

Figure 4 simulates the profile of infected and activated macrophages for young and old mice. Initially there are more activated macrophages in the lungs of old mice (in response to enhanced IFN-γ). However this later becomes reversed as antigen specific responses are generated in young mice, resulting in more activated macrophages in the lungs of young mice up to day 30 of infection; thereafter the number of macrophages in the lungs of old mice again becomes increased. Both densities stabilize after 40 days of infection. The density profiles of infected macrophages for young and old mice intersect in a similar manner to the profiles of the bacterial load. Experimental data is unavailable for these profiles, however based upon the equations and bacterial load described above we can predict that old mice will accumulate more macrophages within the lung than young mice as infection progresses.

Figure 5 shows the concentration of IFN-γ for young and old mice. Old mice initially have more IFN-γ within the lungs, attributed to enhanced $CD8^+$ T cell activity, which models experimental observations in [23] and [26]. This early response creates a 'bump' in the graph. Note that this early activity by $CD8^+$ T cells does not correlate to an increase in cells numbers for this subset. Responsiveness is independent of $CD8^+$ T cell proliferation and considered to be enhanced activity of a resident activated cell population within the lungs of old mice [26]. This early response is transient, after which the source of IFN-γ is antigen specific $CD4^+$ and $CD8^+$ T cells. The delay in generation of antigen specific immunity in old mice leads to a cross-over between young and old mice at approximately 30-40 days, which is in line with experimental observations [23] and [26].

Figure 6 shows IL-12 levels, with a significant early increase in IL-12 production by old mice compared to young, which has been observed experimentally in [26].

Figure 7 shows that the IL-2 concentration in old mice is less than in young mice; this has been experimentally verified in [4], in conjunction with data in [8].

Figure 8 shows the densities of T cells for young and old mice. Both profiles stabilize around day 60. Based upon experimental data [23], the density of $CD8^+$ T cells for old mice is always less than for young mice. However, for $CD4^+$ T cells there is a crossover: old mice initially

have fewer $CD4^+$ T cells during the first 28-40 days of infection. This is a consequence of delayed/defective generation of antigen specific immunity specifically within the $CD4^+$ T cell subset ([23], [13] and unpublished observations). This agrees with measurements given in [24], [23], and [26].

The profile of IL-10 (not shown here) has the same features as in Figure 3, namely, initially it is lower in old mice, but eventually increases to levels above that seen in young mice.

5 Simulation Experiments

The model that we have developed corroborated experimental data. We therefore used our model to determine whether immunity against *M. tuberculosis* infection in old mice could be enhanced if $CD4^+$ T cell numbers/function were increased. In our first experiment, we increased IL-2 driven proliferation and determined the bacterial load within the lung. Increasing k_{13} by 25%, 50% and 70% resulted in a reduction of the bacterial load within the lungs of old mice of 3%, 9%, and 24% respectively (Figure 9 a)). For young mice this reduction was more considerable. Increasing k_{13} by 20%, 40% and 46% resulted in a reduction of the bacterial load by 5%, 19%, and 38% respectively (data not shown).

The second experiment determined the effect of increasing the activation status of $CD4^+$ T cells for old mice by increasing the rate λ_z of MHCII activation. Increasing λ_z by 25%, 50% and 100% resulted in a reduction of the bacterial load by 4%, 9% and 23% respectively (Figure 9 b)). Similarly to the above, increasing the activation rate of $CD4^+$ T cells in young mice led to a more profound effect. Increasing λ_z by 20%, 40% and 70% resulted in a reduction of the bacterial load by 6%, 13%, and 42% respectively (data not shown).

Our simulations therefore demonstrate that protective immunity can be enhanced in old mice by increasing the activation status or proliferation of $CD4^+$ T cells within the lung, leading to improved antigen specific T cell IFN-γ production and macrophage activation. In contrast to young mice however, the decrease in bacterial load within the lungs of old mice was moderate suggesting that other age-associated defects contribute to failing immunity in old age.

6 Conclusions

The elderly are more susceptible to many infectious diseases, including tuberculosis [2], [17], [18], [21], [25]. Increasing susceptibility is highly associated with the loss or delay in the generation of antigen specific $CD4^+$ T cell mediated immunity [8], [11]. For tuberculosis, where antigen specific $CD4^+$ T cell derived IFN-γ is essential [5], such a loss can lead to a significant delay or failure to control infection. The murine model has been an essential tool for the determination of immune function during infection with *M. tuberculosis*. Infection is initiated when *M. tuberculosis* bacillus enters *resting* macrophages within the lung, stimulating macrophages to secrete IL-12 and present antigen to $CD4^+$ and $CD8^+$ T cells in the context of MHC molecules [5]. Specific interactions between macrophages and T cells leads to the secretion of IFN-γ by T cells which *activate* macrophages to control or kill *M. tuberculosis* [5]. This mechanism prevents mycobacterial replication and each activated macrophage contains a small number of mycobacteria. A failure to adequately activate macrophages leads to *infected* macrophages that harbor replicating mycobacteria which can eventually burst and release *M. tuberculosis* into the extracellular environment [5]. In young mice, antigen specific T cell secretion of IFN-γ is required to activate macrophages. IFN-γ can be derived from $CD4^+$ or $CD8^+$ T cells; however $CD4^+$ T cell responses always dominate. The generation of antigen specific T cells in young mice requires 2-3 weeks to be detected within the lung after which T cell IFN-γ production stabilizes in parallel to the bacterial load [5]. In contrast, old mice fail to generate antigen specific T cell responses within the lung until 3-4 weeks after infection, which results in an increased bacterial load within the lung at this time [23], [4]. This

altered response is a result of age associated changes in T cell function [8], [11] leading to a delay in or suboptimal generation of immunity. Changes in T cell function with increasing age are partly a result of thymic atrophy, leading to reduced output of naive T cells in addition to an increase in homeostatic (or antigen) driven expansion of T cells with an effector/memory phenotype [7].

Interestingly, old mice possess a resident population of $CD8^+$ T cells within the lung that can respond independent of antigen and secrete IFN-γ early after infection [26]. IFN-γ secreting $CD8^+$ T cells reside within a population of activated ($CD44^{hi}$) cells that are likely to be specific for a previously encountered antigen and respond during *M. tuberculosis* infection in a bystander fashion [1], [12]. Antigen independent IFN-γ secretion activates macrophages and facilitates early control of infection (initially more activated versus infected macrophages). This response is transient, and the requirement for antigen specific $CD4^+$ T cell IFN-γ is absolute (leading to more infected versus activated macrophages and a higher bacterial burden later). This early innate immune response, in combination with a delayed generation of acquired immunity, leads to a cross-over in the lung bacterial loads. Early infection is associated with fewer bacteria in the lungs of old mice, whereas the delayed generation of acquired immunity results in an eventual increase in the bacterial load compared to young mice [26], as shown in the simulations. The simulations predict that, compared to young mice, old mice will have increased numbers of infected macrophages, $CD4^+$ T cells, and IL-12 within the lung as infection progresses. These predictions can now be validated experimentally using the aged mouse model. The model therefore predicts that old mice succumb to tuberculosis because of overwhelming pulmonary inflammation and cellular involvement (not simply increased bacterial load). Unpublished observations in the laboratory support these predictions. Furthermore, our simulations demonstrate improving the local interaction of $CD4^+$ T cells with antigen presenting cells, or increasing the availability of IL-2 within the lung, has a positive outcome on the course of infection. These findings could have significant consequences on how therapeutic vaccines or therapies are used in the elderly.

Acknowledgement

The project described was supported by the National Science Foundation upon agreement O112050, and, Grant Number R01AG-021097 from the National Institute On Aging. The content is solely the responsibility of the authors and does not necessarily represent the official view of the National Institute On Aging or the National Institute of Health.

References

1. Berg RE, Crossley E, et al. Memory CD8+ T cells provide innate immune protection against Listeria monocytogenes in the absence of cognate antigen. J. Exp. Med 2003;198(10):1583–93. [PubMed: 14623912]
2. Centers for Disease Control and Prevention. Reported tuberculosis in the United States. Atlanta, GA: 2005.
3. Cooper AM, Magram J, Ferrante J, Orme IM. Interleukin 12 (IL-12) is crucial to the development of protective immunity in mice intravenously infected with *Mycobacterium tuberculosis*. J. Exp. Med 1997;186(1):39–45. [PubMed: 9206995]
4. Cooper AM, Callahan JE, Griffin JP, Roberts AD, Orme IM. Old mice are able to control low-dose aerogenic infections with *Mycobacterium tuberculosis*. Infect. Immun 1995;63(9):3259–65. [PubMed: 7642254]
5. Flynn JL, Chan J. Immunology of tuberculosis. Annu. Rev. Immunol 2001;19:93–129. [PubMed: 11244032]
6. Flynn JL, Chan J, Triebold KJ, Dalton DK, Stewart TA, Bloom BR. An essential role for interferon gamma in resistance to *Mycobacterium tuberculosis* infection. J. Exp. Med 1993;178(6):2249–54. [PubMed: 7504064]

7. Globerson A, Effros RB. Ageing of lympocytes and lymphocytes in the aged. Immunology Today 2000;21(10):215–220.
8. Haynes L, Linton PJ, Eaton SM, Tonkonogy SL, Swain SL. Interleukin 2, but not other common gamma chain-binding cytokines, can reverse the defect in generation of CD4 effector T cells from naive T cells of aged mice. J. Exp. Med 1999;190(7):1013–24. [PubMed: 10510091]
9. Junqueira-Kipnis AP, Turner J, Gonzalez-Juarrero M, Turner OC, Orme IM. Stable T-cell population expressing an effector cell surface phenotype in the lungs of mice chronically infected with *Mycobacterium tuberculosis*. Infection and Immunology 2004;72(1):570–575.
10. Levin M, Newport MJ, et al. Familial disseminated atypical mycobacterial infection in childhood: a human mycobacterial susceptibility gene? Lancet 1995;345(8942):79–83. [PubMed: 7815885]
11. Linton PJ, Haynes L, Tsui L, Zhang X, Swain S. From naive to effector–alterations with aging. Immunol Rev 1997;160:9–18. [PubMed: 9476661]
12. Lertmemongkolchai G, Cai G, et al. Bystander activation of CD8+ T cells contributes to the rapid production of IFN-gamma in response to bacterial pathogens. J. Immunol 2001;166(2):1097–105. [PubMed: 11145690]
13. Orme IM. Aging and immunity to tuberculosis: increased susceptibility of old mice reflects a decreased capacity to generate mediator T lymphocytes. J. Immunol 1987;138(12):4414–8. [PubMed: 3495592]
14. Orme IM, Griffin JP, Roberts AD, Ernst DN. Evidence for a defective accumulation of protective T cells in old mice infected with *Mycobacterium tuberculosis*. Cell Immunol 1993;147(1):222–9. [PubMed: 7681730]
15. Orme IM. The kinetics of emergence and loss of mediator T lymphocytes acquired in response to infection with *Mycobacterium tuberculosis*. J. Immunol 1987;138(1):293–8. [PubMed: 3097148]
16. van Pinxteren LA, Cassidy JP, Smedegaard BH, Agger EM, Andersen P. Control of latent *Mycobacterium tuberculosis* infection is dependent on CD8 T cells. Eur. J. Immunol 2000;30(12): 3689–98. [PubMed: 11169412]
17. Rajagopalan S. Tuberculosis and aging: a global health problem. Clin. Infect. Dis 2001;33(7):1034–9. [PubMed: 11528577]
18. Rajagopalan S, Yoshikawa TT. Tuberculosis in long-term-care facilities. Infect. Control. Hosp Epidemiol 2000;21(9):611–5. [PubMed: 11001270]
19. Sud D, Bigbee C, Flynn JL, Kirschner DE. Contribution of $CD8^+$ T cells to control of *Mycobacterium tuberculosis* infection. The Journal of Immunology 2006;176:4296–4314. [PubMed: 16547267]
20. Serbina NV, Flynn JL. Early emergence of CD8(+) T cells primed for production of type 1 cytokines in the lungs of *Mycobacterium tuberculosis*-infected mice. Infect. Immun 1999;67(8):3980–8. [PubMed: 10417164]
21. Schultz M, Hernandez JM, et al. Onset of tuberculosis disease: new converters in long-term care settings. Am. J. Alzheimers Dis. Other. Demen 2001;16(5):313–8. [PubMed: 11603168]
22. Turner J, Gonzalez-Juarrero M, Ellis DL, Basaraba RJ, Kipnis A, Orme IM, Cooper AM. In vivo IL-10 production reactivates chronic pulmonary tuberculosis in C57BL/6 mice. J. Immunol 2002;169 (11):6343–51. [PubMed: 12444141]
23. Turner J, Frank AA, Orme IM. Old mice express a transient early resistance to pulmonary tuberculosis that is mediated by CD8 T cells. Infect. Immun 2002;70(8):4628–37. [PubMed: 12117976]
24. Turner J, Orme IM. The expression of early resistance to an infection with Mycobacterium tuberculosis by old mice is dependent on IFN type II (IFN-γ) but not IFN type I. Mech. Ageing Dev 2004;125(1):1–9. [PubMed: 14706232]
25. Thrupp L, Bradley S, et al. Tuberculosis prevention and control in long-term-care facilities for older adults. Infect. Control Hosp. Epidemiol 2004;25(12):1097–108. [PubMed: 15636299]
26. Vesosky B, Flaherty DK, Turner J. Th1 cytokines facilitate CD8-T-cell-mediated early resistance to infection with *Mycobacterium tuberculosis* in old mice. Infection and Immunity 2006;74(6):3314–3324. [PubMed: 16714559]
27. Vesosky B, Flaherty DK, Rottinghaus EK, Bemaer GL, Turner J. Age dependent increase in early resistance of mice to *Mycobacterium tuberculosis* is associated with an increase in CD8 T cells that are capable of antigen independent IFN-γ production. Experimental Gerontology 2006;41(11):1185–1194. [PubMed: 17029663]

28. Vesosky B, Turner J. The influence of age on immunity to infection with *Mycobacterium tuberculosis*. Immunological Reviews 2005;205:229–243. [PubMed: 15882357]

29. Wigginton JE, Kirschner DE. A model to predict a cell-meadiated immune regulatory mechanism during human infection with *Mycobacterium tuberculosis*. The Journal of Immunology 2001;166:1951–1967. [PubMed: 11160244]

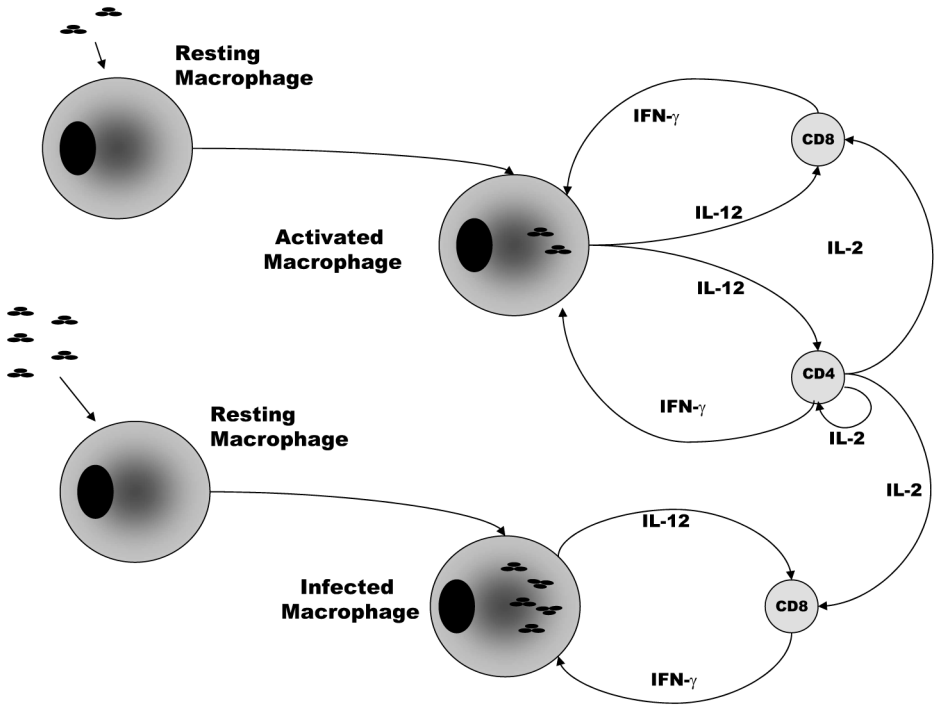

Figure 1.

Activated and infected macrophages present antigen to T cells via MHC molecules and, in combination with IL-12, stimulate $CD4^+$ and $CD8^+$ T cells to secrete IFN-*γ*; IFN-*γ* activates infected macrophages and enables them to control infection.

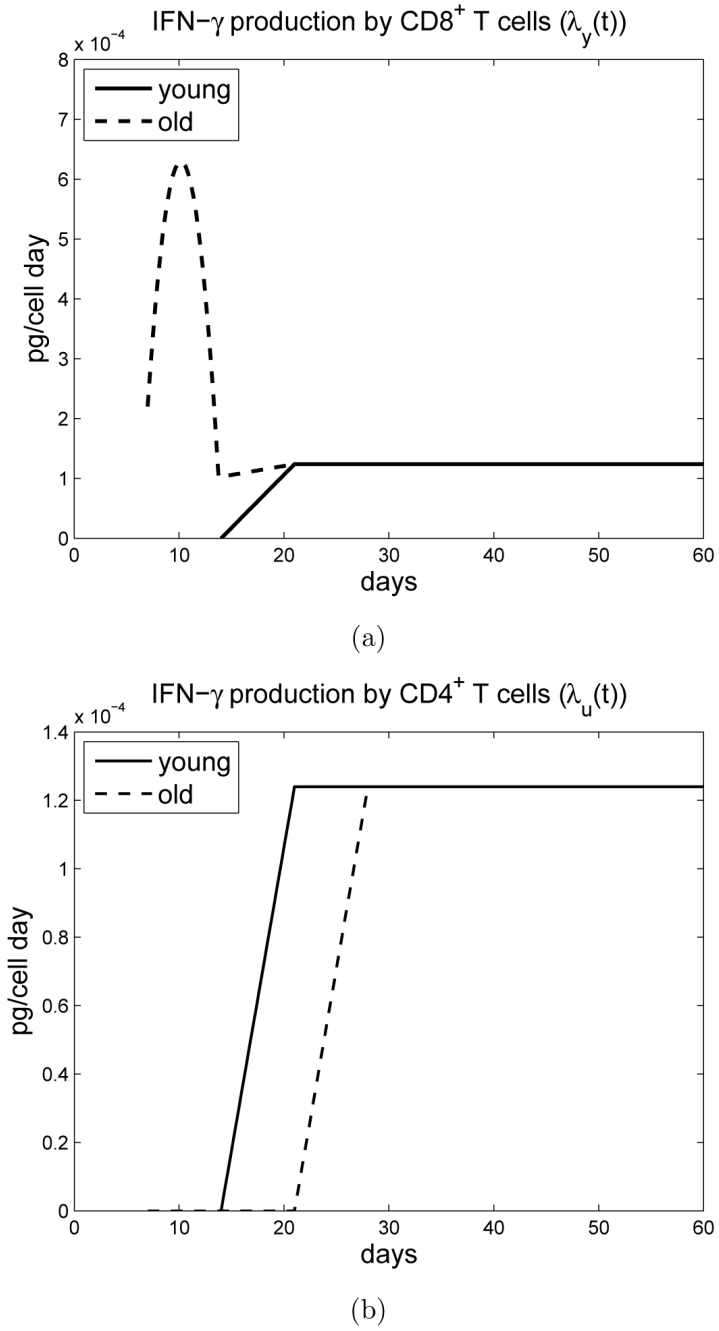

Figure 2.

a) Time-dependent IFN-γ production rate $\lambda_y(t)$ by $CD8^+$ T cells for young and old mice. b) Time-dependent IFN-γ production rate $\lambda_u(t)$ by $CD4^+$ T cells for young and old mice.

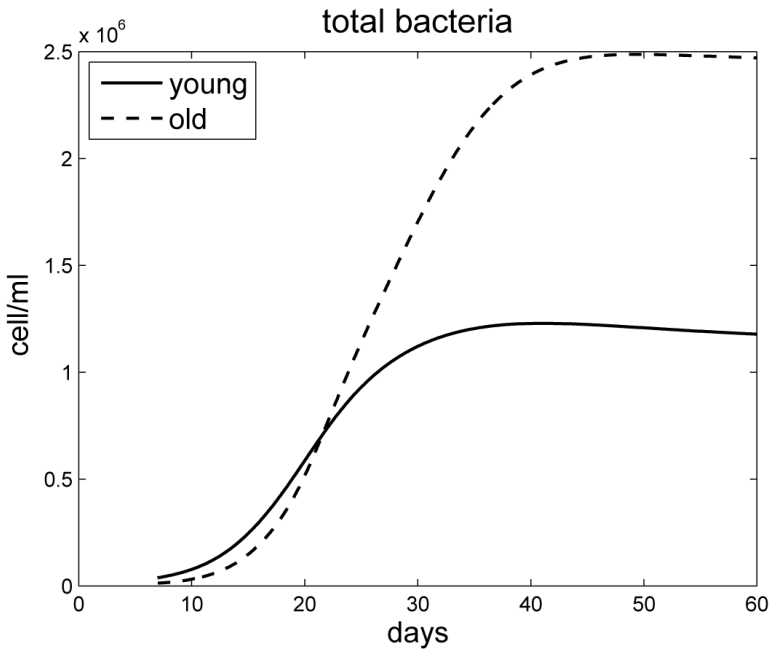

Figure 3.
The bacterial load for young and old mice

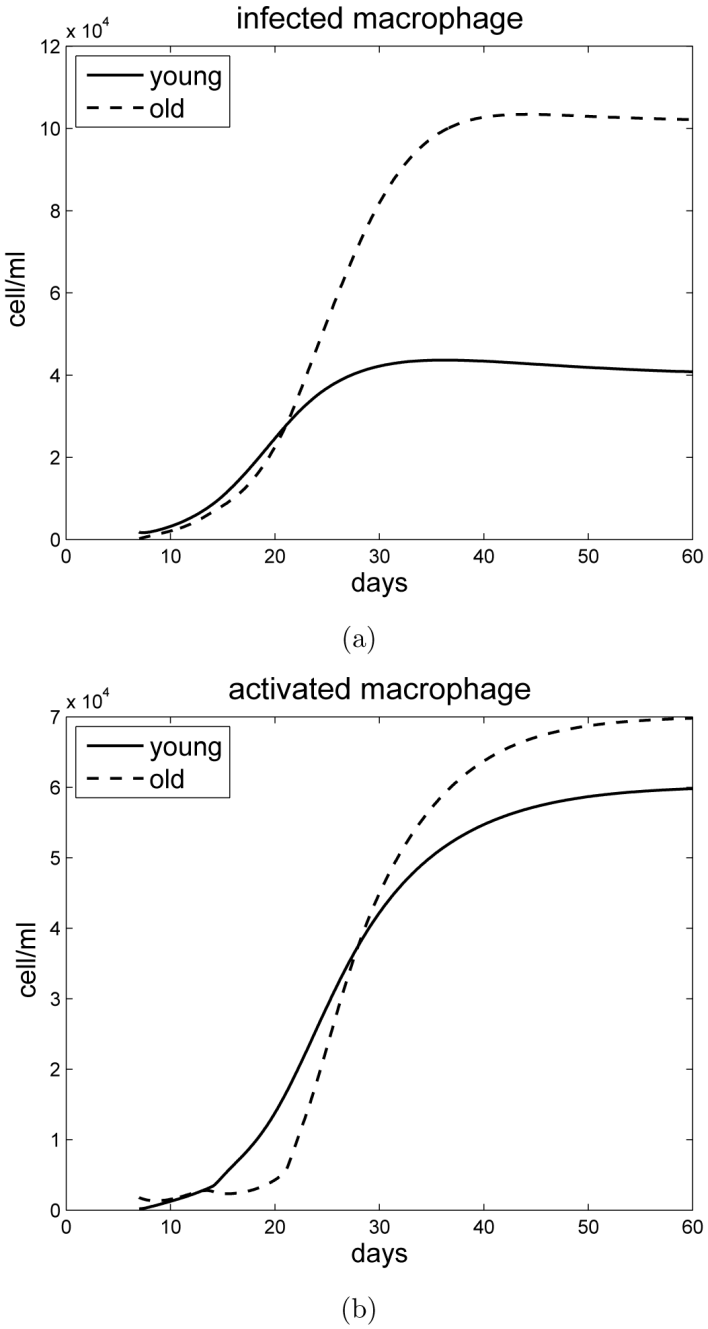

Figure 4.
a) Simulation of infected macrophages in young and old mice. b) Simulation of activated macrophages in young and old mice.

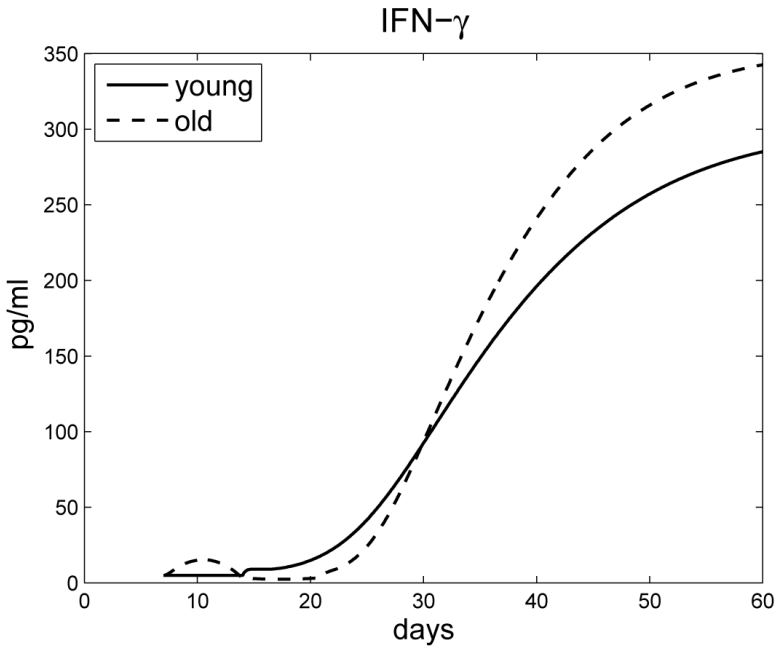

Figure 5.
Concentration of IFN-*γ* in young and old mice.

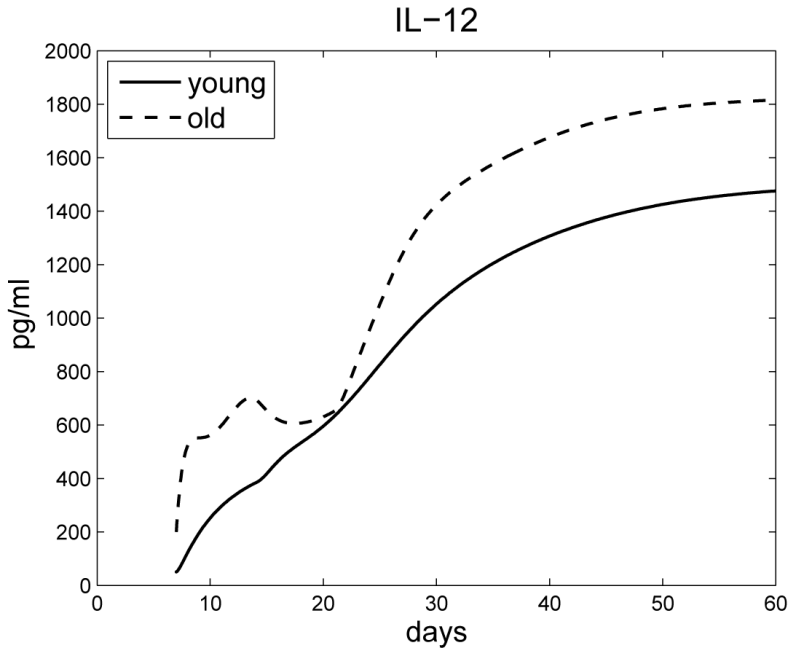

Figure 6.
Concentration of IL-12 in young and old mice.

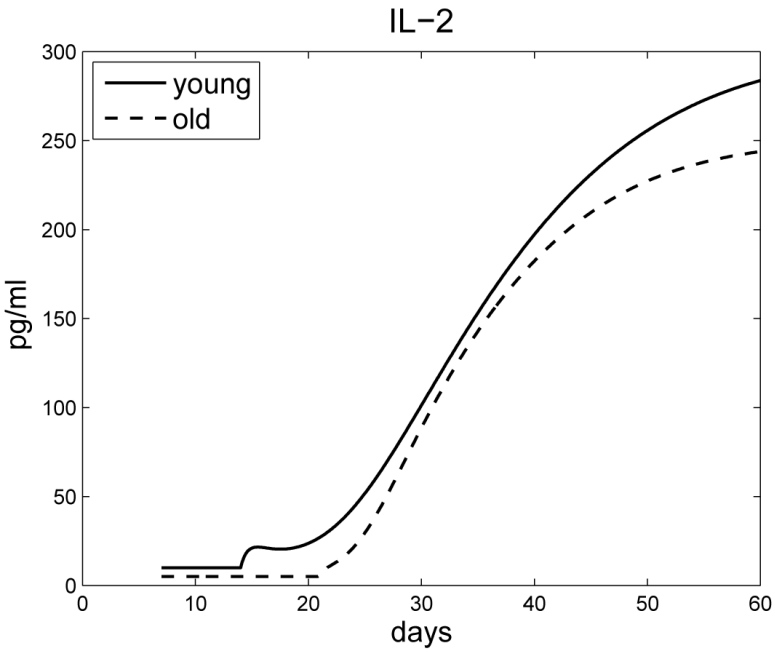

Figure 7.
The profile of IL-2 for young and old mice.

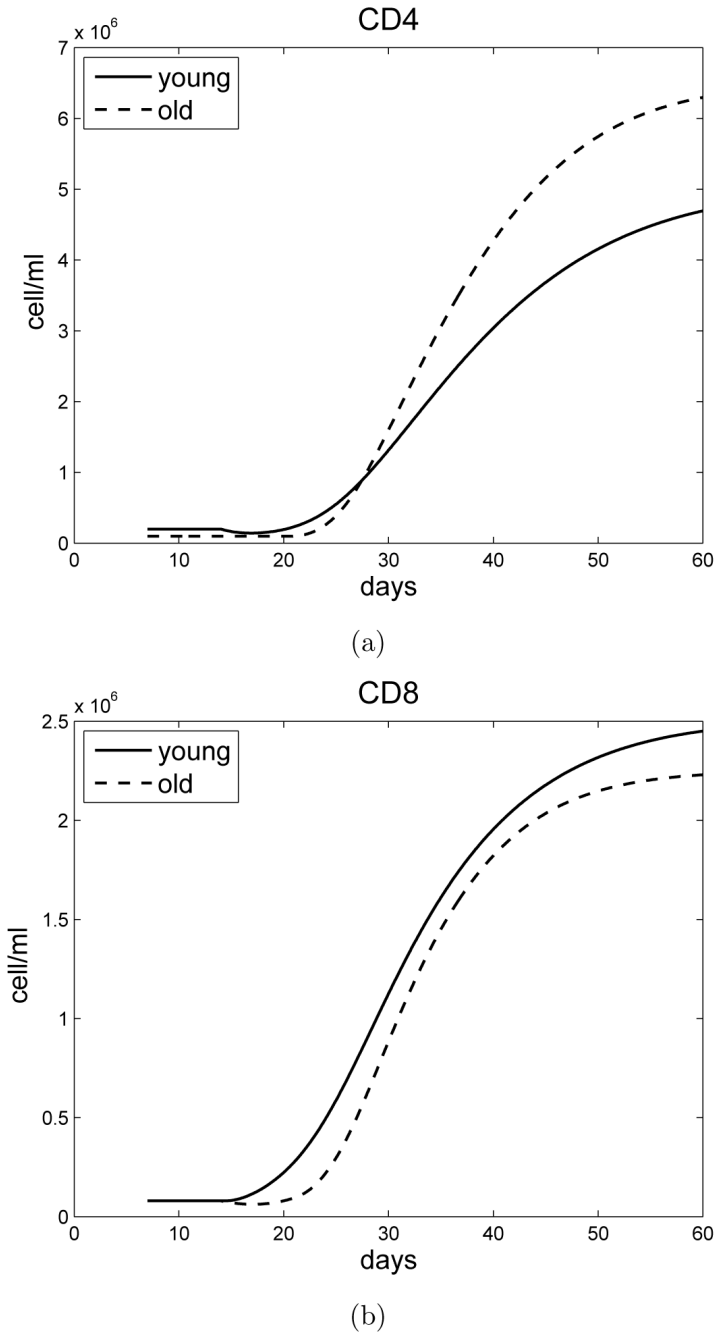

Figure 8.
a) The densities of $CD4^+$ T cells in young and old mice. b) The densities of $CD8^+$ T cells in young and old mice.

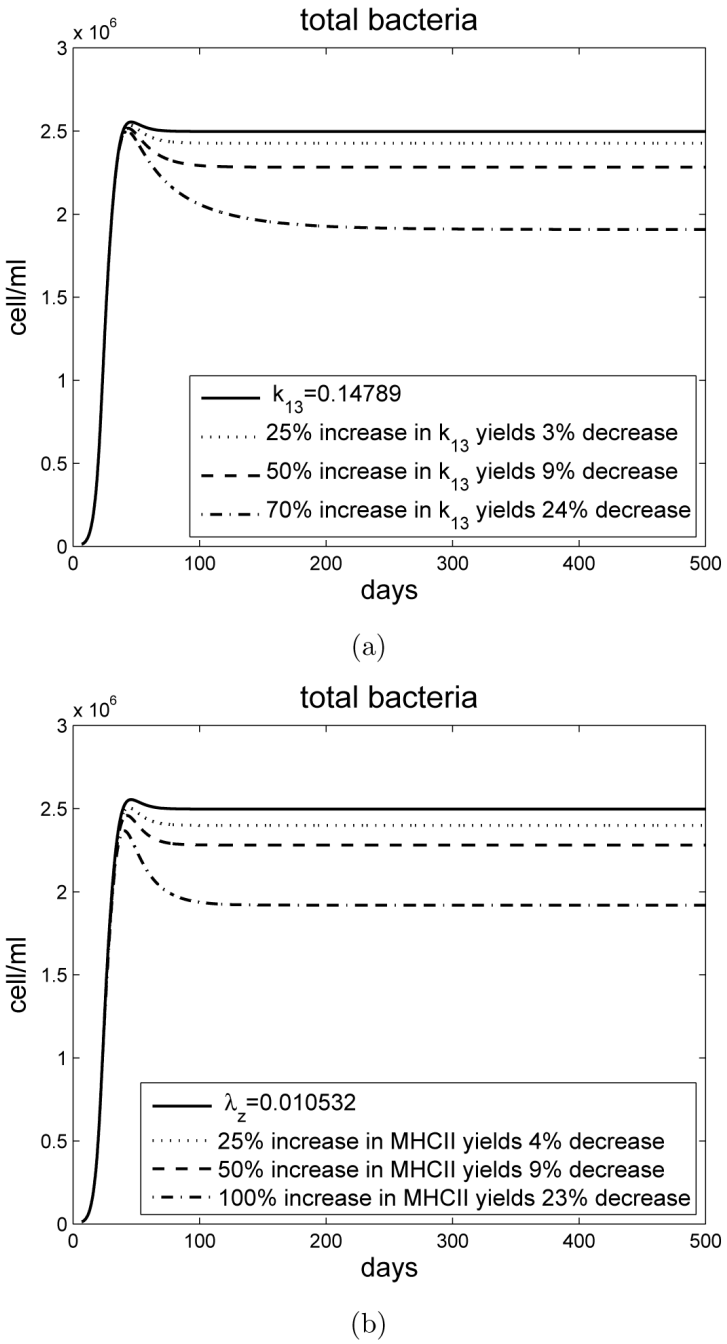

Figure 9.

a) Simulation experiment for old mice with varying the rate of proliferation of $CD4^+$ T cells by IL-2. The bacterial load decreases as the rate of k_{13} activation is increased. b) Simulation experiment for old mice with varying the rate of MHCII activation. The bacterial load decreases as the rate of MHCII activation is increased.

Table 1

Model variables and their initial values at day 7 for young and old mice. The choice of the initial values is explained in the last paragraph of Section 3.

		young	old	units
T_4	density of $CD4^+$ T cells	2×10^5	10^5	cell/ml
T_8	density of $CD8^+$ T cells	8×10^4	8×10^4	cell/ml
M_R	density of resting macrophages	5×10^5	5×10^5	cell/ml
M_I	density of infected macrophages	1800	200	cell/ml
M_A	density of activated macrophages	200	1800	cell/ml
B_I	density of bacteria residing in infected macrophages	36 000	4000	cell/ml
B_A	density of bacteria residing in activated macrophages	1000	9000	cell/ml
B_E	density of extracellular bacteria	1000	1000	cell/ml
I_γ	concentration of IFN-γ	5	5	pg/ml
I_2	concentration of IL-2	10	5	pg/ml
I_{10}	concentration of IL-10	100	50	pg/ml
I_{12}	concentration of IL-12	50	200	pg/ml

Table 2

Model parameters and their explanation.

α_I	growth rate of B_I
α_E	growth rate of B_E
α_A	growth rate of B_A
k_1	rate of infection of resting macrophages
k_2	burst rate of infected macrophages
k_3	activation rate of infected macrophages
k_4	deactivation rate of activated macrophages
k_5	take up of B_E by activated macrophages
k_6	rate of activation of resting macrophages
k_7	IL-10 production rate by infected macrophages
k_8	IL-12 production rate by activated macrophages
k_9	IL-12 production rate by resting macrophages
k_{10}	IL-2 production rate by T_4
k_{11}	loss of IL-2 due to proliferation of T_4
k_{12}	loss of IL-2 due to proliferation of T_8
k_{13}	rate of proliferation of T_4 by IL-2
k_{14}	rate of proliferation of T_8 by IL-2
c_1	saturation for infection of resting macrophages
c_2	saturation for activation of infected macrophages
c_3	IFN-γ inhibition for deactivation of activated macrophages
c_4	saturation for deactivation of activated macrophages
c_5	TB saturation for activation of resting macrophages
c_6	IFN-γ saturation for activation of resting macrophages
c_7	saturation for IL-10 inhibition by IL-10
c_8	saturation for IL-12 inhibition by IL-10
c_9	saturation for IL-12 production by resting macrophages
c_{10}	saturation for T cell proliferation by IL-2
c_{11}	saturation for IFN-γ production by T cells and IL-12
N	maximal carrying capacity of an infected macrophage
n_1	average number of B_I in an infected macrophage
n_2	average number of B_A in an activated macrophage
n_3	threshold at which a resting macrophage becomes infected
μ_{MA}	death rate of activated macrophages
μ_{MI}	death rate of infected macrophages
μ_{10}	decay rate of IL-10
μ_{12}	decay rate of IL-12
μ_2	decay rate of IL-2
μ_γ	decay rate of IFN-γ
μ_{T4}	death rate of T_4
μ_{T8}	death rate of T_8
$*\lambda_u$	rate of IFN-γ production by T_4
$*\lambda_v$	rate of IFN-γ production by T_8
$*\lambda_z$	rate of MHCII activation
$*\lambda_x$	rate of MHCI activation

Table 3

Parameter values for young and old mice. The abbreviation u. o. stands for unpublished observations.

coeffcient	young	old	source
α_I	0.5 day^{-1}	0.5 day^{-1}	[13]
α_E	0 day^{-1}	0 day^{-1}	[13]
α_A	0 day^{-1}	0 day^{-1}	this work
k_1	0.4 day^{-1}	0.4 day^{-1}	this work
k_2	0.81139 day^{-1}	0.81139 day^{-1}	this work
k_3	0.023415 day^{-1}	0.025440 day^{-1}	[26]
k_4	0.28876 day^{-1}	0.61707 day^{-1}	[13]
k_5	8.1301 $\times 10^{-5}$ ml/cell day	8.1301 $\times 10^{-5}$ ml/cell day	this work
k_6	0.077068 day^{-1}	0.13539 day^{-1}	[26]
k_7	0.50610 pg/ml cell	0.55044 pg/ml cell	this work
k_8	0.28503 pg/cell day	0.53162 pg/cell day	this work
k_9	5×10^{-4} pg/cell day	0.001 pg/cell day	[26]
k_{10}	2.1873 $\times 10^{-4}$ pg/cell day	1.7301 $\times 10^{-4}$ pg/cell day	[4]
k_{11}	1.6383 $\times 10^{-4}$ pg/cell day	1.4788 $\times 10^{-4}$ pg/cell day	this work
k_{12}	1.6383 $\times 10^{-5}$ pg/cell day	1.413 $\times 10^{-5}$ pg/cell day	this work
k_{13}	0.1638 ml/pg day	0.14789 ml/pg day	[8]
k_{14}	0.01638 ml/pg day	0.01413 ml/pg day	[8]
c_1	10^6 cell/ml	10^6 cell/ml	[13]
c_2	50 pg/ml	50 pg/ml	this work
c_3	3	3	this work
c_4	1 pg/ml	1 pg/ml	[13]
c_5	10^5 cell/ml	10^5 cell/ml	[13]
c_6	20 pg/ml	20 pg/ml	this work
c_7	5000 pg/ml	5000 pg/ml	this work
c_8	200 pg/ml	200 pg/ml	this work
c_9	5000 cell/ml	5000 cell/ml	[13]
c_{10}	50 pg/ml	50 pg/ml	this work
c_{11}	50 cell/ml	50 cell/ml	this work
M_R	5×10^5 cell/ml	5×10^5 cell/ml	u. o.
N	25	25	u. o. & [13]
n_1	20	20	u. o.
n_2	5	5	u. o.
n_3	10	10	u. o.
μ_{MA}	0.015 day^{-1}	0.015 day^{-1}	u. o.
μ_{MI}	0.2 day^{-1}	0.2 day^{-1}	u. o.
μ_{10}	7.23 day^{-1}	7.23 day^{-1}	[13]
μ_{12}	1.188 day^{-1}	1.188 day^{-1}	[13]
μ_2	1.188 day^{-1}	1.188 day^{-1}	u. o.
μ_γ	3 day^{-1}	3 day^{-1}	[13]
μ_{T4}	0.33 day^{-1}	0.33 day^{-1}	[13]
μ_{T8}	0.33 day^{-1}	0.33 day^{-1}	[13]
$*\lambda_u$	1.24 $\times 10^{-4}$ pg/cell day	1.24 $\times 10^{-4}$ pg/cell day	[29] & this work
$*\lambda_y$	1.24 $\times 10^{-5}$ pg/cell day	1.24 $\times 10^{-4}$ pg/cell day	this work
$*\lambda_z$	0.010532 ml/pg day	0.010532 pg/cell day	this work
$*\lambda_x$	0.005266 ml/pg day	0.0022854 pg/cell day	this work